

The origin of stiffening in cross-linked semiflexible networks

P. R. Onck, T. Koeman, T. van Dillen, E. van der Giessen¹

¹*Micromechanics of Materials, Materials Science Centre, Nijenborgh 4, 9747 AG Groningen, The Netherlands*

Strain stiffening of protein networks is explored by means of a finite strain analysis of a two-dimensional network model of cross-linked semiflexible filaments. The results show that stiffening is caused by non-affine network rearrangements that govern a transition from a bending dominated response at small strains to a stretching dominated response at large strains. Thermally-induced filament undulations only have a minor effect; they merely postpone the transition.

PACS numbers: 87.16.Ka, 87.15.La, 82.35.Lr

There is a deep interest in the mechanical response of biological tissues and gels in view of the importance for biological functions such as cell motility and mechanotransduction. Many network-like biological tissues respond to deformation by exhibiting an increasing stiffness, i.e. ratio between change of stress and change of strain. This has been demonstrated by micropipette and microtwisting experiments [1] on individual cells and through rheological experiments on in-vitro gels of cytoskeletal filaments (actin, vimentin, keratin [2, 3, 4] and neuronal intermediate filaments [5]), as well as on fibrin [6, 7]. These biological gels fall within the class of *semiflexible* polymers, which has also attracted much theoretical attention in the last decade [8, 9, 10, 11, 12]. However, these theoretical studies have primarily focused on the small-strain regime, tractable for analytical treatment.

In a simple conceptual view, a biopolymer network is an *interlinked* structure of *filaments*. Thus, stiffening can result from stiffening of the polymeric filaments between cross-links, from alterations in the network structure, or both. The current paradigm is that stiffening is primarily due to the stiffening of the filaments themselves. This idea has been worked out in detail very recently by Storm *et al.* [5] by adopting the worm-like chain model for actin filaments in combination with the assumption that the network deforms in an affine manner, i.e., each filament is assumed to follow the overall deformation. The worm-like chain model is a well-documented description for the stretching of semiflexible polymers, where the longitudinal stiffness of undulated filaments is attributed primarily to bending; the axial stiffness of the polymeric chain itself is much higher [8, 13]. As the filament is stretched (at constant temperature), the amplitude of the transverse thermal undulations reduces and, as a consequence, the stiffness increases. In the limit that the filament is pulled straight, all subsequent axial deformation would have to originate from axial straining of the chain, but at an enormous energy cost. Given this description of individual filaments, Storm *et al.* [5] proceed by considering a network consisting of infinitely many filaments. Initially the filaments are randomly orientated, and as the sample is deformed the network is assumed to distort in an affine manner. The affine deformation assumption is well known in network models for rubber elasticity, and allows for a relatively simple description of the overall network response on the basis of the behavior of a single filament. The small-

strain affine deformation assumption in two-dimensional networks of straight filaments has recently been studied in great detail by Head *et al.* [11], who conclude that its validity depends on the cross-link density of the filaments. Their conclusion, however, cannot be immediately transferred to the stiffening results of Storm *et al.* since it applies only to the initial response.

In contrast with the cited literature, we demonstrate in this paper that stiffening lies in the network rather than in its constituents. During deformation, the filaments rotate in the direction of straining, which induces a transition from a bending-dominated response to one that is controlled by stretching of aligned filaments. By comparing cross-linked networks with and without thermal undulations, we show that filament reorientation is the dominant mechanism, while the thermal undulations only postpone the onset of stiffening.

Our model is a two-dimensional network model of filaments in a periodic unit cell of dimensions $W \times W$. The network is generated by randomly placing filaments with length L at random orientations inside the cell, with proper account of periodicity. Thermal undulations are mimicked by superposing on each filament transverse normal modes of the type $b_n \sin(n\pi x/L)$, where the amplitudes b_n follow a Gaussian distribution (cf. [14]) with standard deviation $\sqrt{2/(l_p L)}(L/n\pi)^2$. The persistence length l_p , i.e., the distance over which the filaments appear straight, is expressed as $l_p \propto \kappa/(k_B T)$ in terms of the bending stiffness κ of the filaments, Boltzmann's constant k_B and temperature T . Clearly, the filaments are straight in case the temperature is low or the bending stiffness is high. We use the first 10 normal modes to generate the initial geometry of the filaments and treat l_p as an independent quantity. During mechanical loading, thermal effects are no longer taken into account.

Points where filaments overlap are considered to be cross-links, similar to the procedure used by Head *et al.* [11] and Wilhelm and Frey [12]. The networks generated by this procedure are taken as the initial, stress-free configuration. In the calculations, the cross-links are assumed to be stiff, so that both displacement and rotation of the two filaments at the cross-link point remain the same. The filaments are elastic rods, characterized by a stretching stiffness μ (axial force [15] needed to induce a unit axial strain) and a bending stiffness κ (bending moment needed to induce a unit radius of curvature).

For isotropic elastic rods these values are related through their cross-sectional geometry, but are treated here as independent. The density of the network is characterized by the line density ρ , i.e., the total length of filaments in the unit-cell divided by the cell area, W^2 . For networks with straight filaments ($l_p/L \rightarrow \infty$), the average distance between cross-links, l_c , is inversely proportional to ρ through $l_c = \pi/\rho$ [16]. We consider networks of different densities, but only above the rigidity percolation threshold [12].

For the numerical study we use the finite element method, discretizing each filament with 10 equal-sized Euler-Bernoulli beam elements accounting for stretching and bending. Geometry changes are accounted for by an updated Lagrangian finite strain formulation. All filaments are perfectly bonded to rigid top and bottom plates, with the top plate displaced horizontally relative to the bottom plate over a distance ΓW , corresponding to an applied shear strain Γ . The macroscopic shear stress τ is calculated from the total horizontal reaction force at the top, divided by W . Convergence studies ensured that the cell size W does not affect the results.

The parameters governing the system are τ , Γ , μ , κ , L , ρ and l_p . We choose to present the results through the following dimensionless parameters: $\bar{\tau} = \tau L/\mu$, Γ , $\bar{\rho} = \rho L$, $\bar{l}_p = l_p/L$ and $\bar{l}_b = \sqrt{\kappa/(\mu L^2)}$. Note that \bar{l}_b is a measure for the 'floppiness' of the filaments, which reduces to the slenderness ratio (thickness over length) for isotropic elastic rods, and \bar{l}_p sets the initial shape of the filaments.

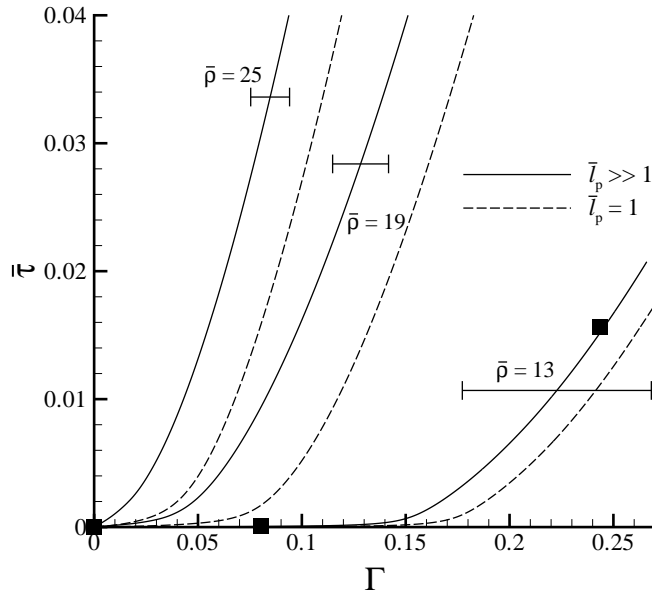


FIG. 1: Average stress ($\bar{\tau}$) versus strain (Γ) response for networks with $\bar{l}_b = 2.3 \times 10^{-4}$ and $\mu/L = 1.6$ MPa at three different densities $\bar{\rho}$ and for straight ($\bar{l}_p >> 1$) and undulated ($\bar{l}_p = 1$) filaments. The error bars have a length of two times the standard deviation in strain at a given Γ for ten different realizations at each density. The squares correspond to three instances during deformation for which the network geometry is shown in Fig. 2.

In a first set of calculations we take $\bar{l}_b = 2.3 \times 10^{-4}$ and $\mu/L = 1.6$ MPa (representative for actin microfilaments [17])

with a density of $\bar{\rho} = 13$, which is well above the rigidity percolation threshold of $\bar{\rho} = 5.7$ [12]. The persistence length is taken to be much larger than the filament length ($\bar{l}_p >> 1$), corresponding to straight filaments. Figure 1 shows the stress-strain response (averaged over ten different random realizations). Three regimes can be identified: a regime with a relatively low stiffness $d\bar{\tau}/d\Gamma$, a transition regime and a high-stiffness regime. Figure 2 shows three snapshots of the $\bar{\rho} = 13$ network geometry at $\Gamma = 0$, 0.08 and 0.24 for a typical realization close to the average response (see the solid squares in Fig. 1). Comparison of Fig. 2b with Fig. 2a reveals that many initially straight filaments have deformed by bending, which corresponds to the characteristic low stiffness at small strain levels for these densities [11, 12]. Subsequently, during the transition regime, percolations of stretched filaments appear that connect the top and bottom of the cell along a $\sim 45^\circ$ direction, Fig. 2c. These filaments are loaded in axial tension, resulting in a higher overall stiffness. Thus, Figs. 2b to 2c demonstrate the transition from a bending dominated regime at small strains (total mechanical energy of the systems primarily consists of bending energy) to a stretching dominated regime at higher strain levels (total energy dominated by the axial stretching energy).

The stress-strain response for two higher densities, $\bar{\rho} = 19$ and 25, is included in Fig. 1. The standard deviation in strain from ten realizations is approximately independent of the stress value for a given density. The scatter in strain, defined as the ratio between the standard deviation and the average, is independent of the density and has a value of approximately 0.2. Figure 1 shows that a certain stress level is achieved at smaller strains in case the network is denser. The network thus gets stiffer with increasing density, while the transition from bending to stretching becomes less abrupt and occurs at smaller strain levels.

Next, the effect of thermally-induced undulations is investigated. The same parameters are used as before, but now we use $\bar{l}_p = 1$, in accordance with experimental findings for actin filaments [17]. Changing the persistence length from $l_p \gg L$ to $l_p = L$ is physically similar to increasing the temperature from 0K to 293K before cross-linking and loading the network instantaneously. Figure 3 depicts the initial geometry for a network where the initial filaments' end-to-end vectors have the same location and orientation as shown in Fig. 2a. The stress-strain results included in Fig. 1 (dashed lines) show that the thermal undulations do not change the shape of the overall stress-strain curve, but merely delay the transition from bending to stretching. The associated 'delay' strain at an applied strain level of $\Gamma = 0.25$ is 0.018, 0.029 and 0.024 for $\bar{\rho} = 13$, 19 and 25, respectively. Similar values were found for densities up to 38. Clearly, only a small fraction of the total strain is due to the presence of thermally-induced undulations.

To make connection with the small-strain study by Head et al. [11], we monitor the degree of affinity of the network during straining to large deformations. For this purpose, we

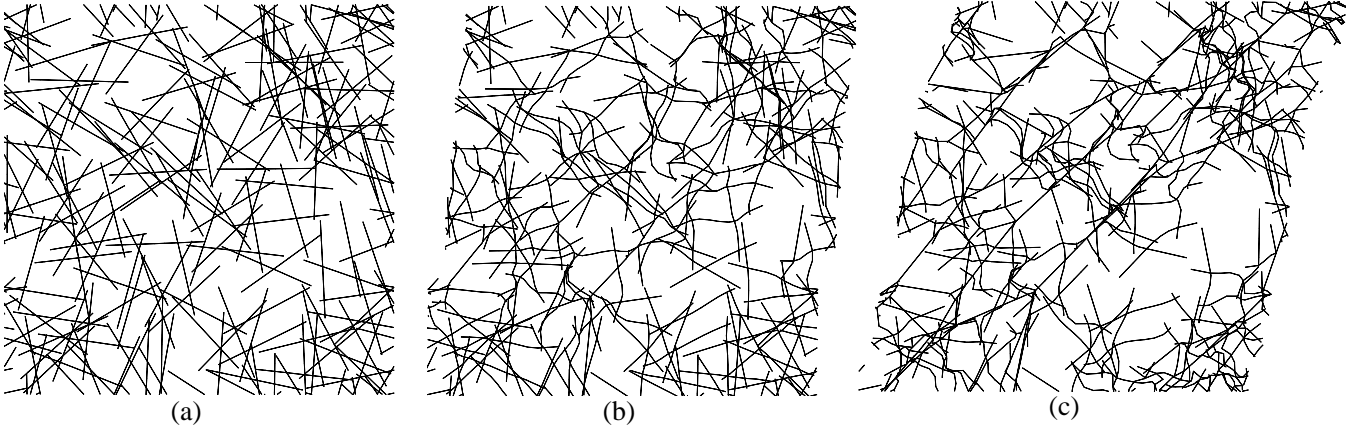


FIG. 2: (a) Initial, $\Gamma = 0$; (b) intermediate, $\Gamma = 0.08$ and (c) large strain, $\Gamma = 0.24$, network configurations for a typical $\bar{p} = 13$ realization close to the average response shown in Fig. 1 (squares).

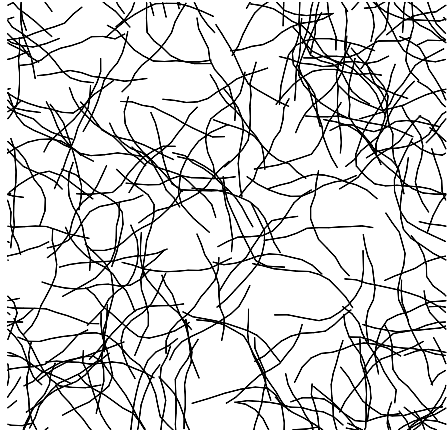


FIG. 3: Initial conformation of a $\bar{p} = 13$ network with undulated filaments corresponding to $\bar{l}_p = 1$.

define the deviation from affine behavior, ΔA , as

$$\Delta A = \frac{1}{n} \sum_{k=1}^n \frac{\|\Delta \mathbf{r}^{(k)} - \Delta \mathbf{r}_{\text{aff}}^{(k)}\|}{\Delta \Gamma \|\mathbf{r}^{(k)}\|}, \quad (1)$$

where $\|\mathbf{r}\|^2 = \mathbf{r} \cdot \mathbf{r}$, n the number of cross-links and $\mathbf{r}^{(k)}$ is the current position vector of cross-link k . $\Delta \mathbf{r}^{(k)}$ is the increment in the position of cross-link k during a shear increment $\Delta \Gamma$ in the simulations, while $\Delta \mathbf{r}_{\text{aff}}^{(k)}$ is the corresponding value were the deformation affine. Figure 4 shows the evolution of ΔA as a function of Γ for the cases shown in Fig. 1. It is observed that the deformation is not affine at small strains, in accordance with [11, 12], while the deformation becomes increasingly affine ($\Delta A \rightarrow 0$) with increasing strain. By comparing Fig. 4 with Fig. 1, we find that in the transition from the bending to the stretching regime, ΔA increases significantly, indicating a reorientation of the filaments. The peak in the $\Delta A - \Gamma$ curve occurs for both straight and undulated filaments in the transition regime. This is another indication of the fact that filament

undulations do not change the nature of network deformation, but merely enhance the strain value at which stretching sets in. Once stretching has set in, the deformation becomes more and more affine.

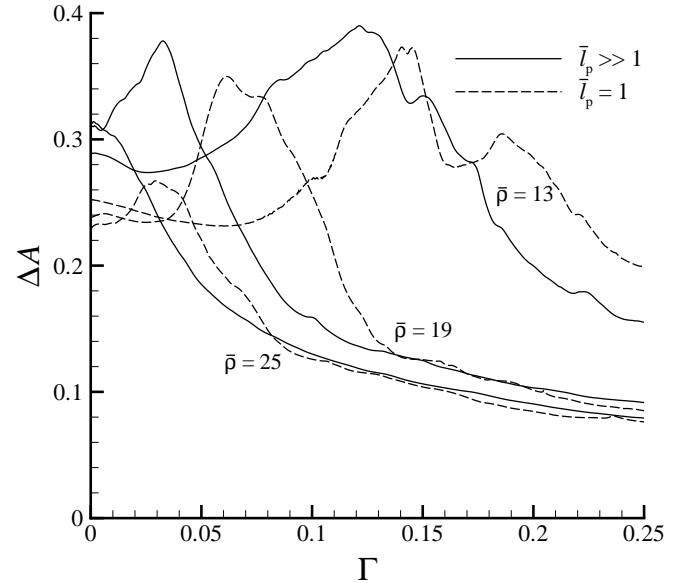


FIG. 4: The deviation from affine behavior, ΔA , as a function of strain, Γ , for $\bar{l}_b = 2.3 \times 10^{-4}$ and $\mu/L = 1.6$ MPa, at three different densities and for straight ($\bar{l}_p \gg 1$) and undulated ($\bar{l}_p = 1$) filaments.

To study the influence of the filament properties, the calculations are repeated, but with a larger bending and stretching stiffness, $\bar{l}_b = 8.3 \times 10^{-4}$ and $\mu/L = 8$ MPa (representative for microtubuli [18]). Note that the bending stiffness increases by a factor of 65, while the stretching stiffness becomes five times larger. Because of the enhanced bending stiffness, the persistence length at the high temperature increases from $\bar{l}_p = 1$ to 65 so that the filaments are almost straight (in accordance with experimental observations on microtubuli [17]). Figure 5 shows the instantaneous shear stiffness, $\bar{G} = d\bar{\tau}/d\Gamma$, as a func-

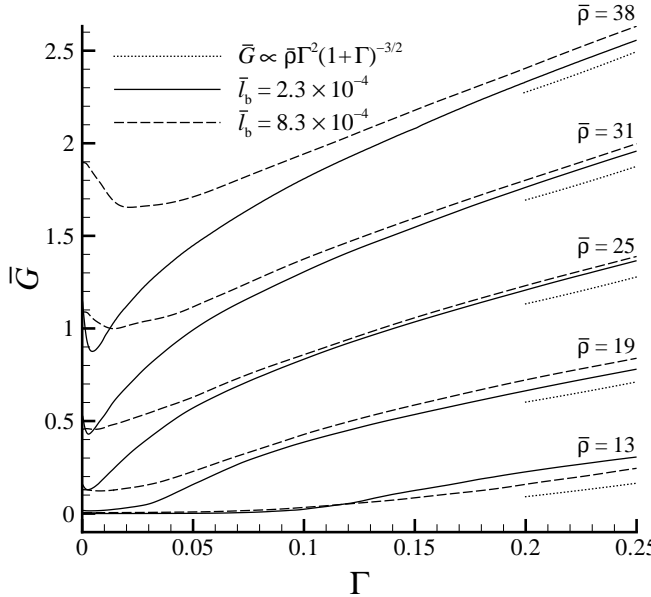


FIG. 5: Shear stiffness as a function of strain for networks with straight filaments having $\bar{l}_b = 2.3 \times 10^{-4}$ or 8.3×10^{-4} . The dotted lines represent the scaling relationship (2), fitted to $\bar{p} = 25$.

tion of shear strain Γ for the two different values of \bar{l}_b (and reference stress μ/L). It can be observed that for the ‘floppy’ filaments ($\bar{l}_b = 2.3 \times 10^{-4}$) the transition from the low-stiffness to the high-stiffness regime shifts to lower strains with increasing density, consistent with Figs. 1 and 4. For densities higher than $\bar{p} = 25$, the transition from bending to stretching is no longer accompanied by severe filament reorientations that cause a peak in ΔA (see Fig. 4), but progresses more smoothly. At higher densities of either floppy or stiff filaments, the stiffness first decreases with strain at small strain levels. This is caused by buckling of filaments oriented at 135° away from the horizontal axis (positive to the right in Fig. 2), which are loaded primarily in compression. Figure 5 also shows that at small strains the overall stiffness for the floppy filaments is much lower than that of the stiffer filaments, but converges to the same value at larger strains. This reflects that bending is the dominant deformation mode in the low-stiffness regime at small strains, while filament stretching governed by μ dominates at large strains.

When filament stretching is the dominant deformation mechanism, the following scaling arguments hold. The overall stress τ is distributed, on average, over the filaments through the force $F \propto \tau l_c$, where $l_c \propto 1/\rho$ is the ‘mesh size’ of the network. This force causes the filaments to deform axially, yielding an elongation $\delta \propto Fl_c/\mu$, which yields an average strain $\Gamma \propto \delta/l_c$. Substitution yields $\Gamma \propto \tau/(\rho\mu)$ so that $G \propto \rho\mu$. In three dimensions the same scaling relation holds [19]. It should be noted that in the high-stiffness regime, the network ‘locks’ when a number of percolations connects top and bottom. Further straining the network only results in stretching the (fixed number of) percolations. In that case one would expect the stiffness to converge to a fixed ‘steady state’ value.

However, due to non-linear geometrical effects at large strains, the stiffness increases with straining according to [20]

$$\bar{G} \propto \bar{p}\Gamma^2(1+\Gamma)^{-3/2}. \quad (2)$$

This scaling is seen from Fig. 5 to successfully characterize the steady state stretching regime at large strains.

This study leads to the following conclusions. Stiffening of cross-linked semiflexible networks is caused by the transition of a bending-dominated response at small strains to a stretching-dominated response at large strains. This transition is mediated by network rearrangements that are not affine. Filament undulations only have a minor effect; they merely postpone the transition from bending to stretching. Above a density-dependent transition strain, the network stiffness scales linearly with density and the filament’s stretching stiffness, which is expected to hold in three dimensions as well.

- [1] N. Wang and D.E. Ingber, *Biochemistry and Cell Biology*, **73**, 327–335 (1995).
- [2] P.A. Janmey, S. Hvidt, J. Lamb, T.P. Stossel, *Nature* **345**, 89 (1990).
- [3] P.A. Janmey, U. Euteneuer, P. Traub and M. Schliwa, *J. Cell Biol.* **113**, 155 (1991).
- [4] L. Ma, J. Xu, P.A. Coulomb and D.J. Wirtz, *J. Biol. Chem.* **274**, 19145 (1999).
- [5] C. Storm, J.J. Pastore, F.C. MacKintosh, T.C. Lubensky and P.A. Janmey, *Nature* (in press)
- [6] S. Hvidt and K. Heller, In: *Physical Networks: polymers and gels*, Eds. W. Burchard and S.B. Ross-Murphy, Elsevier Applied Science, London, 1990.
- [7] J.V. Shah and P.A. Janmey, *Rheol. Acta* **36**, 262–268 (1997).
- [8] F.C. MacKintosh, J. Käs and P.A. Janmey, *Phys. Rev. Lett.* **75**, 4425 (1995).
- [9] H. Isambert and A.C. Maggs, *Macromolecules* **29**, 1036–1040 (1996).
- [10] D.C. Morse, *Phys. Rev. E*, **58**, R1237 (1998).
- [11] D.A. Head, A.J. Levine and F.C. MacKintosh, *Phys. Rev. E*, **68**, 061907 (2003).
- [12] J. Wilhelm and E. Frey, *Phys. Rev. Lett.* **91**, 108103 (2003).
- [13] Bending energy is internal energy, but since the bending inside a filament is induced by transverse thermal undulations, the stiffness according to the worm-like chain model is often referred to as ‘entropic stiffness’. It should, however, be distinguished from the classical entropy elasticity in flexible polymers.
- [14] J. Käs, J. Strey, H. Tang, J.X. Finger, D. Ezzel, R. Sackmann, E. Janmey, P.A. Janmey, *Biophys. J.*, vol. 70, 609–625, 1996.
- [15] All quantities with dimension force are computed per unit out-of-plane thickness.
- [16] G. Pike and C. Seager, *Phys. Rev. B* **10**, 1421 (1974).
- [17] Howard, J., *Mechanics of motor proteins and the cytoskeleton*, Sinauer Associates, Inc., Sunderland, Massachusetts, 2001.
- [18] Consider a microtubule (MT) having an inner radius of 8 nm and an outer radius of 12 nm. If we compare the stretching and bending stiffness with that of an actin microfilament (MF), represented by a solid rod of radius 4 nm, it follows that $\mu_{MT}/\mu_{MF} = 5$, $\kappa_{MT}/\kappa_{MF} = 65$.
- [19] In three dimensions we have $F \propto \tau l_c^2$ and $l_c \propto 1/\sqrt{\rho}$, leading again to $G \propto \rho\mu$.

[20] Consider a ‘network’ consisting of parallel percolated filament strings that are initially normal to the shear plane and a distance $\propto 1/\rho$ apart. The strings only have an axial stiffness μ . Upon application of a shear strain, the strings only rotate initially, but when straining proceeds and the strings rotate by an

angle $\beta = \tan^{-1} \Gamma$, they have to stretch, thus leading to an increase of the overall stiffness. Straightforward mechanics yields $G \propto \rho \mu \cos \beta \sin^2 \beta = \rho \mu \Gamma^2 (1 + \Gamma)^{-3/2}$, leading to Eq. (2). The same scaling holds in three dimensions.